

# Cyclotriphosphazene as a Dendritic Core for the Preparation of Columnar Supermolecular Liquid Crystals

Joaquín Barberá,<sup>†</sup> Josefina Jiménez,<sup>\*,‡</sup> Antonio Laguna,<sup>‡</sup> Luis Oriol,<sup>\*,†</sup> Sonia Pérez,<sup>‡</sup> and José Luis Serrano<sup>†</sup>

*Polymer and Liquid Crystal Group, Química Orgánica, Instituto de Ciencia de Materiales de Aragón, Universidad de Zaragoza-C.S.I.C., 50009 Zaragoza, Spain, and Departamento de Química Inorgánica, Instituto de Ciencia de Materiales de Aragón, Universidad de Zaragoza-C.S.I.C., 50009 Zaragoza, Spain*

Received May 16, 2006. Revised Manuscript Received September 7, 2006

A series of supermolecular liquid crystals has been synthesized by combining a cyclotriphosphazene unit as a dendritic core and polycatenar mesogenic units. Microsegregation of the alkyl chains and the aromatic central cores together with space-filling properties make these cyclophosphazenes adopt a discotic conformation and are assembled in a columnar mesophase. Furthermore, IR spectra taken over a range of temperatures provide evidence that the discotic structure and columnar assembly are highly stabilized by H-bonding. The columnar mesophase can be maintained or vitrified at room temperature depending on the length of the terminal alkyl chains. Structural characterization of these assemblies has been carried out by X-ray diffraction. Helical ordering has been detected in oriented samples of these materials.

## Introduction

Supermolecular liquid crystals are the subject of increasing research as a “bottom-up” approach to the preparation of functional materials with self-organizing properties.<sup>1</sup> This kind of mesogenic material is based on giant molecules that are monodisperse or single, identifiable molecules. Most of the reported supermolecular liquid crystals are based on a dendritic central core upon which mesogenic units are linked. For example, silicon-based inorganic scaffolds have been one of the most widely used central systems; in particular, silsesquioxanes are used as rigid cores to which mesogenic units are attached by means of flexible spacers.<sup>2,3</sup>

Cyclotriphosphazenes are also very attractive in this respect. These compounds are highly versatile molecules with a multiarmed rigid ring that can be used as a core for the exploration of new dendritic structures.<sup>4</sup> Nevertheless, in the field of liquid crystals this kind of structure has hardly been studied. Most of the results described to date concern cyclotriphosphazenes substituted with calamitic mesogenic units which bear a terminal chain and these units are directly linked to the inorganic ring.<sup>5–9</sup> These materials exhibit calamitic phases, which are explained in terms of a model

consisting of mesogenic units arranged approximately perpendicular to the cyclotriphosphazene ring. In this way, the molecule adopts a conformation that resembles a calamitic superstructure capable of being organized in a nematic or smectic phase.<sup>10,11</sup>

On the other hand, the self-organization of dislike molecules into columnar assemblies has received a great deal of attention in materials science.<sup>12</sup> In this field, the self-organizing ability of liquid crystals having a discotic structure has been widely used as the driving force to obtain columnar assemblies of organic and organometallic structures. In particular, compounds that exhibit columnar mesomorphism at room temperature or molecular, mesomorphic glasses having a columnar structure are especially interesting in the design of functional materials.<sup>13</sup>

Very recently, we accomplished the synthesis of columnar cyclotriphosphazenes bearing mesogenic units with three terminal alkyl chains (Figure 1).<sup>14</sup> The microsegregation of the rigid and flexible parts of the system, as well as the space-

\* To whom correspondence should be addressed. L. Oriol: fax, +34 976 762686; e-mail, loriol@unizar.es. J. Jiménez: fax, +34 976 761187; e-mail, jjimvil@unizar.es.

<sup>†</sup> Polymer and Liquid Crystal Group, Química Orgánica.

<sup>‡</sup> Departamento de Química Inorgánica.

- (1) Saez, I. M.; Goodby, J. W. *J. Mater. Chem.* **2005**, *15*, 26.
- (2) Saez, I. M.; Goodby, J. W. *Liq. Cryst.* **1999**, *26*, 1101. Saez, I. M.; Goodby, J. W. *J. Mater. Chem.* **2001**, *11*, 2845.
- (3) Saez, I. M.; Goodby, J. W.; Richardson, R. M. *Chem. Eur. J.* **2001**, *7*, 2758.
- (4) Majoral, J. P.; Caminade, A. M. *Chem. Rev.* **1999**, *99*, 845 and references therein.
- (5) Moriya, K.; Suzuki, T.; Kawanishi, Y.; Masuda, T.; Mizusaki, H.; Nakagawa, S.; Ikematsu, H.; Mizuno, K.; Yano, S.; Kajiwara, M. *Appl. Organomet. Chem.* **1998**, *12*, 771–779 and references therein.
- (6) Moriya, K.; Suzuki, T.; Yano, S.; Kajiwara, M. *Liq. Cryst.* **1995**, *19*, 711–713.

- (7) Moriya, K.; Suzuki, T.; Yano, S.; Kajiwara, M. *Trans. Mater. Res. Soc. Jpn.* **1999**, *24*, 481–484.
- (8) Moriya, K.; Kawanishi, Y.; Yano, S.; Kajiwara, M. *Chem. Commun.* **2000**, 1111–1112.
- (9) Moriya, K.; Ikematsu, H.; Nakagawa, S.; Yano, S.; Negita, K. *Jpn. J. Appl. Phys.* **2001**, *40*, L340–L342.
- (10) Levelut, A. M.; Moriya, K. *Liq. Cryst.* **1996**, *20*, 119.
- (11) Moriya, K.; Suzuki, T.; Yano, S.; Miyajima, S. *J. Phys. Chem. B* **2001**, *105*, 7920.
- (12) Kumar, S. *Chem. Soc. Rev.* **2006**, *35*, 83–109.
- (13) See for instance: (a) Percec, V.; Glodde, M.; Bera, T. K.; Miura, Y.; Shiyonovskaya, I.; Singer, K. D.; Balagurusamy, V. S. K.; Heiney, P. A.; Schnell, I.; Rapp, A.; Spiess, H. W.; Hudson, S. D.; Duan, H. *Nature* **2002**, *419*, 384–387 and references therein. (b) Piris, J.; Debije, M. G.; Stutzmann, N.; Laursen, B. W.; Pisula, W.; Watson, M. D.; Björnholm, T.; Müllen, K.; Warman, J. M. *Adv. Funct. Mater.* **2004**, *14*, 1053. (c) Pisula, W.; Kastler, M.; Wasserfallen, D.; Robertson, J. W. F.; Nolde, F.; Kohl, C.; Müllen, K. *Angew. Chem., Int. Ed.* **2006**, *45*, 819–823 and references therein. (d) Lehmann, M.; Köhn, C.; Meier, H.; Renker, S.; Oelhof, A. *J. Mater. Chem.* **2006**, *16*, 441–451 and references therein.

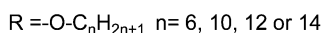
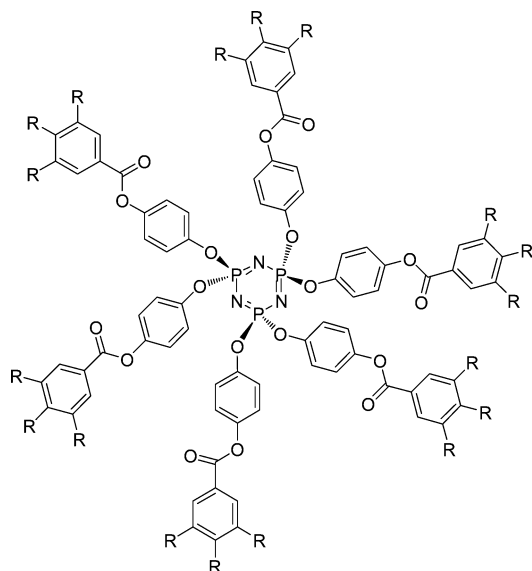


**Figure 1.** Chemical structure of the columnar cyclotriphosphazenes described in ref 14.

filling properties, drive the organization of the dendritic supermolecules in the mesomorphic state. The columnar mesomorphism was explained in terms of an arrangement of the mesogenic units approximately parallel to the inorganic ring. The formation of both rodlike and disclike gross shapes in these supermolecules is due to the conformational freedom on the P–O–Ar bonds linking the mesogenic units to the central rigid core. Furthermore, as pointed out by Saez and Goodby, the shorter the linking unit, the more likely the material will act as a single supermolecular entity since the introduction of spacers will allow the mesogenic groups to dominate the overall properties.<sup>1</sup>

In this paper we report the synthesis and properties of a new series of supermolecules based on organic cyclotriphosphazenes bearing amide groups in the peripheral mesogenic units. The incorporation of amide groups was carried out to increase the intermolecular forces between the cyclotriphosphazenes through hydrogen bonding. In fact, one-dimensional columns of discotic liquid crystals are formed through self-assembly of discotic mesogens and these columnar assemblies can be held together more strongly by means of hydrogen bonding of mesogens.<sup>15</sup> A detailed study of the thermal and structural properties of these materials is also included.

## Results and Discussion

**Synthesis and Characterization.** The specific reaction sequences used for phosphazene cyclic trimers **3–5** are described in Figure 2. Hexachlorocyclotriphosphazene was reacted with excess 4-acetamidophenol in the presence of  $K_2CO_3$  in acetone to yield trimer **1**. The 4-acetamidophenoxy units of trimer **1** were hydrolyzed to 4-aminophenoxy groups

with sodium hydroxide in methanol to give **2**. Treatment of trimer **2** with an excess of the corresponding acid chloride (1.3 mol/mol of  $NH_2$ ), in the presence of  $NEt_3$  in THF, led to trimers **3–5**. Compound **2** was previously described by Allcock et al. starting from the 4-nitrophenoxy derivative by catalytic reduction with hydrogen.<sup>16</sup>

All cyclic phosphazene trimers **1–5** were characterized by IR,  $^1H$  NMR,  $^{31}P\{^1H\}$  NMR, and  $^{13}C\{^1H\}$  NMR spectroscopy, mass spectrometry (LSIMS or MALDI-TOF techniques), and microanalytical data. The IR spectra of all these compounds display peaks at around  $1200\text{ cm}^{-1}$  (br) (P=N) and  $960\text{ cm}^{-1}$  (P–O)<sup>17</sup> (see Experimental Section). The carbonyl stretching peak of trimer **1** was observed at  $1668\text{ cm}^{-1}$  and this disappears after hydrolysis. Reaction of **2** with the acid chloride gave rise to a new band at around  $1645\text{ cm}^{-1}$  (C=O), which shows the success of the condensation reaction. The IR spectra for all trimers also show the absorptions attributable to  $\nu(N-H)$ . The  $^{31}P\{^1H\}$  NMR spectra consist of a singlet in all cases, indicating hexasubstitution, with the signals having almost identical chemical shifts (ca. +10.5 ppm) because the phosphorus environments are not significantly different. These positions are also similar to those observed for other hexa(phenoxy)cyclotriphosphazenes.<sup>18</sup> The  $^1H$  and  $^{13}C\{^1H\}$  NMR spectra are also consistent with the formulas indicated. Thus, in addition to the hydrogen atoms on the aromatic ring (AA'BB' spin system), the proton spectrum of **1** displays a signal for the acetyl protons at 2.04 ppm and a signal for the NH proton at 9.92 ppm, both of which are replaced by a signal at 4.46 ppm (br) ( $NH_2$  protons) after hydrolysis. In trimers **3–5**, the resonance for the NH proton is observed at around 8.9 ppm. The aromatic hydrogens of the  $OC_6H_4N$  groups show two somewhat distorted "pseudodoublets" (a deceptively simple pattern arising from the strictly speaking AA'BB' spin system) with apparent coupling constants ( $N = J_{AB} + J_{AB'}$ ) in the range 6.9–8.4 Hz. These latter spectra also show resonances corresponding to the other two equivalent aromatic protons and to the hydrogen atoms of the three terminal chains (see Experimental Section for details). The signals in the  $^{13}C\{^1H\}$  NMR spectra were assigned by comparison with those observed for other similar compounds.<sup>14</sup> Microanalytical data are summarized in the Experimental Section. Compounds **1** and **2** retain water molecules even after drying in vacuo at  $40\text{ }^\circ\text{C}$  for 48 h, as evidenced by microanalytical and mass spectral data (LSIMS technique in a nitrobenzyl alcohol matrix). The complete reaction of all peripheral amine groups and the single molecular nature of the trimers **3–5** was also checked by size exclusion chromatography and MALDI-TOF mass spectrometry (using dithranol-NaI as matrix), which confirmed the expected chemical structure (see Figure 3 as an example).

**Mesomorphic and Thermal Properties.** The thermal and mesomorphic properties of the cyclotriphosphazenes **3–5** were studied by thermogravimetry (TGA), differential scan-

(14) Barberá, J.; Bardají, M.; Jiménez, J.; Laguna, A.; Martínez, M. P.; Oriol, L.; Serrano, J. L.; Zaragoza, I. *J. Am. Chem. Soc.* **2005**, *127*, 8994–9002.

(15) Bushey, M. L.; Nguyen, T. Q.; Zhang, W.; Horoszewski, D.; Nuckolls, C. *Angew. Chem., Int. Ed.* **2004**, *43*, 5446–5453.

(16) Allcock, H. R.; Austin, P. E.; Rakowsky, T. F. *Macromolecules* **1981**, *14*, 1622–1625.

(17) Allcock, H. R. *J. Am. Chem. Soc.* **1964**, *86*, 2591.

(18) Allcock, H. R.; Connolly, M. S.; Sisko, J. T.; Al-Shali, S. *Macromolecules* **1988**, *21*, 323–334.

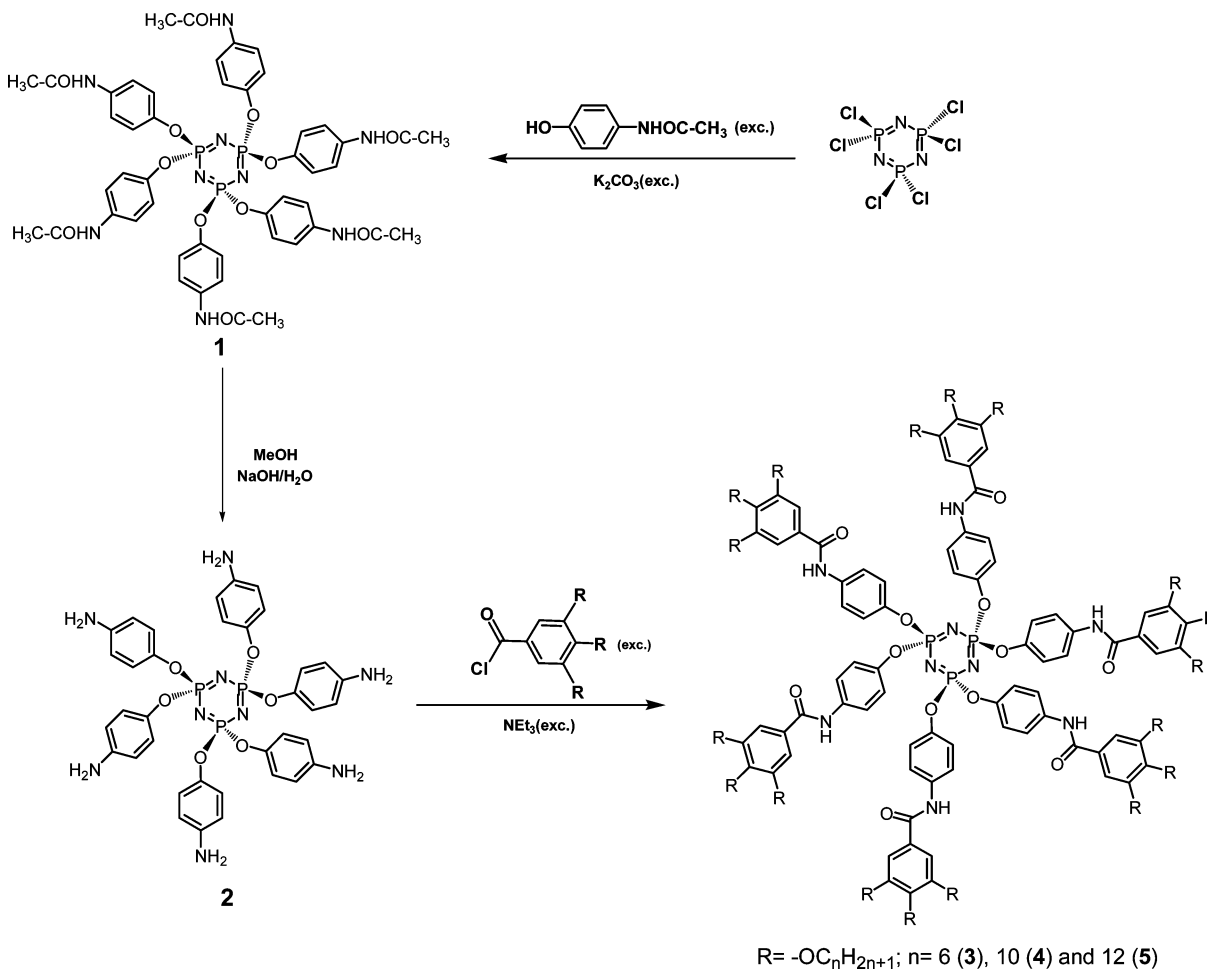


**Figure 2.** Chemical structure and synthetic pathway of cyclotriphosphazenes 3–5.

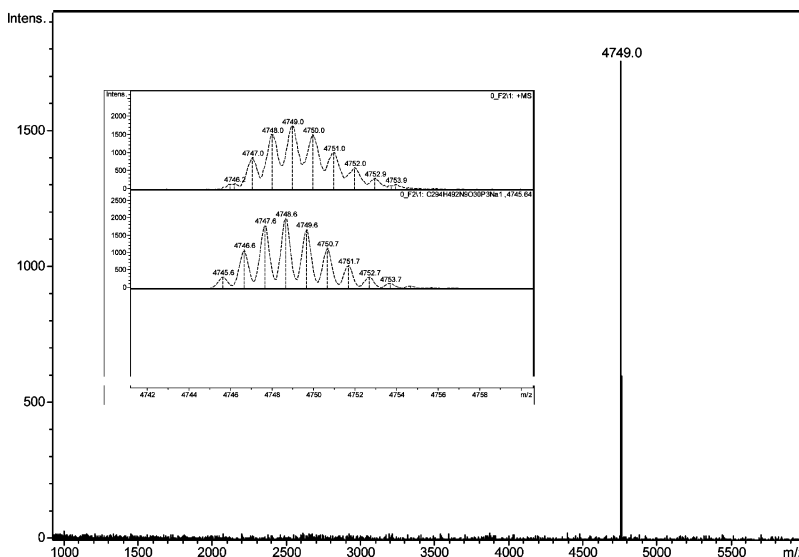


**Figure 3.** MALDI-TOF mass spectrum of **5** (matrix: dithranol + NaI). See inset: experimental isotopic pattern (up) and theoretical isotopic pattern (down).

ning calorimetry (DSC), polarized-light optical microscopy (POM), and X-ray diffraction (see below) and the results are summarized in Table 1. These cyclotriphosphazenes exhibit a high thermal stability, as deduced from the thermogravimetric curves. The compounds are thermally stable up to a temperature close to 325 °C in an inert atmosphere and exhibit a sharp thermal decomposition with a maximum degradation temperature at around 370 °C.

Furthermore, the presence of volatiles is ruled out on the basis of the weight loss curves. The high thermal stability of organophosphazenes is well-known<sup>19</sup> and has made these inorganic dendritic scaffolds good candidates for the preparation of thermally stable dendritic materials.

The mesomorphic behavior of these materials, which were obtained as powdery samples, strongly depends on the length of the terminal alkyl chains. Cyclophosphazene **3**, which

**Table 1. Thermal Properties and Phase Transitions for Cyclotriphosphazenes 3–5**

compound	2% <sup>a</sup>	$T_{\text{onset}}^a$	$T_{\text{max}}^a$	phase transitions <sup>b</sup> ( $\Delta H$ kJ/mol)
<b>3</b>	329	346	363	K 132 (38.1) Col <sub>h</sub> 177 (5.5) I <sup>c</sup>
<b>4</b>	338	349	369	g 61 Col <sub>h</sub> 171 (6.7) I <sup>d</sup>
<b>5</b>	341	351	377	K 6 (112.3) Col <sub>r</sub> 87 (13.9) Col <sub>h</sub> 137 (7.9) I

<sup>a</sup> Thermogravimetric data: Temperature corresponding to 2% weight loss;  $T_{\text{onset}}$  corresponds to the onset of the decomposition detected on the weight loss curve and  $T_{\text{max}}$  was read at the maximum of the derivative thermogravimetric curve. <sup>b</sup> Transition temperature, in °C, detected from the DSC second heating scan (10 °C/min) and read at the maximum of the peak due to the broadness of the peaks.  $\Delta H$  in kJ/mol.  $T_g$  was detected as the half-height point of the baseline jump. <sup>c</sup> Sample previously annealed at 110 °C for 1 h (see text). <sup>d</sup> Sample previously annealed at 80 °C for 1 h (see text).

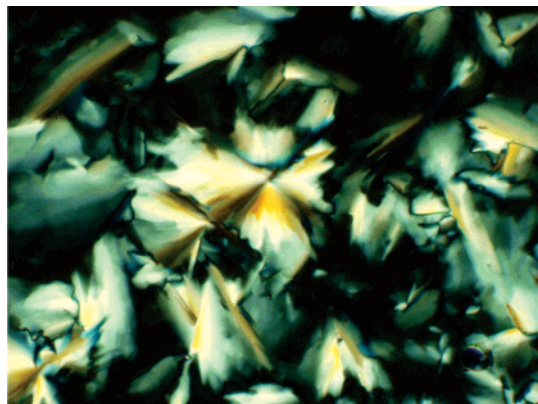


**Figure 4.** Microphotograph of cyclotriphosphazene **3** cooled from the I state (10 °C/min) and taken at 155 °C.

contains hexyloxy chains, was obtained as a glassy material that, on heating, exhibited a  $T_g$  at around 70 °C followed by a cold crystallization (detected at about 110 °C) and finally melting to give a mesomorphic material at around 130 °C. This mesophase was difficult to identify on this first heating run due to the high viscosity of the cyclotriphosphazene. However, cooling from the isotropic state (detected above ca. 180 °C), a well-defined pseudo focal-conic fan-shaped texture together with homeotropic regions was clearly observed by POM; this texture is consistent with a hexagonal columnar phase (see Figure 4). Other phase transitions were not observed on further cooling either by DSC or POM, and the texture was retained at room temperature in a molecular mesomorphic glass.<sup>20</sup> A subsequent heating run showed a glass transition was followed by cold crystallization, melting, and isotropization transitions, which were again detected at similar temperatures to those observed in the first heating run. These results provide evidence of a slow tendency to crystallize and this was further confirmed when a sample of this compound was annealed at 110 °C for 1 h. Indeed, the DSC heating trace of this sample showed a melting transition at 132 °C followed by an isotropization transition at 177 °C.

Cyclotriphosphazene **4**, which bears decyloxy terminal chains, was also obtained as a glassy material and exhibited a  $T_g$  at around 60 °C. However, in contrast to **3**, cold

crystallization was not detected above the  $T_g$  and the DSC traces only showed an endothermic peak at around 170 °C, corresponding to isotropization. On cooling of the sample, typical textures for a Col<sub>h</sub> mesophase were observed and, as in the case of **3**, these textures were retained at room temperature in a vitrified solid material. To ascertain the tendency of this compound to crystallize, the sample was annealed at a temperature above  $T_g$  ( $T_{\text{annealing}} = 80$  °C). However, the annealed sample exhibited only a glass transition and an isotropization transition, a situation that demonstrates that crystallization did not take place. This thermal behavior is surprising, bearing in mind that compound **4** has a similar structure to compound **3**, and also demonstrates the influence of the length of the alkyl chains in the packing of this kind of unconventional mesogens.

Compound **5** was obtained as a powdery, partially crystalline sample according to the first heating run. An endothermic peak was detected in this scan at about 70 °C, and this followed by two small endothermic peaks at around 85 and 135 °C. This latter transition corresponds to the mesophase–isotropic state transition. A clearer characterization was achieved in the cooling process. At around 135 °C, both by POM and DSC, an isotropic phase–mesophase transition was detected. Furthermore, the textures were clearly assigned to a Col<sub>h</sub> mesophase and exhibited a spontaneous tendency to homeotropic orientation, especially if the sample was cooled down slowly (Figure 5a). A new phase transition was observed on subsequent cooling at around 85 °C in the DSC scan. A subtle change in texture was also detected in the POM study. The homeotropic regions changed at about this temperature and exhibited a slight birefringence (Figure 5b). However, the nature of this columnar mesophase cannot be unambiguously assigned (see below). The compound eventually crystallized at temperatures below room temperature. On subsequent heating scans, the melting transition was observed at about 5 °C.

Comparison of the thermal behavior of these materials with the homologous cyclotriphosphazenes bearing ester groups<sup>14</sup> reveals that amide derivatives exhibit a much wider mesophase range. This trend is a consequence of the stabilization of the interactions between mesogens through hydrogen bonding.<sup>21</sup> Indeed, the presence of a large number of aliphatic chains causes the molecules to adopt a discotic structure.<sup>14</sup> Furthermore, the microsegregation of peripheral aliphatic chains and rigid central cores favors aggregation into columns. This assembly is highly stabilized by H-bonding between the central aromatic units,<sup>22</sup> as recently proposed for similar three-armed organic compounds.<sup>23</sup>

(19) de Jaeger, R.; Gleria, M. *Prog. Polym. Sci.* **1998**, *23*, 179–276 and references therein.

(20) Wedler, W.; Demus, D.; Zaszke, H.; Mohr, K.; Schäfer, W.; Weissflog, W. *J. Mater. Chem.* **1991**, *1*, 347. Kürschner, K.; Strohrriegel, P. *Liq. Cryst.* **2000**, *27*, 159.

(21) See for instance: (a) Brienne, M. J.; Gabard, J.; Lehn, J. M.; Stibor, I. *J. Chem. Soc., Chem. Commun.* **1989**, *24*, 1868–1870. (b) Paleos, C. M.; Tsiourvas, D. *Angew. Chem., Int. Ed. Engl.* **1995**, *34*, 1696–1711. (c) Brunsveld, L.; Zhang, H.; Glasbeck, M.; Vekemans, J. A. J. M.; Meijer, E. W. *J. Am. Chem. Soc.* **2000**, *122*, 6175–6182.

(22) (a) Guchi, F.; Nicola, G. D.; Franz, H.; Gottarelli, G.; Mariani, P.; Bossi, M. G. P.; Spada, G. P. *J. Am. Chem. Soc.* **1994**, *116*, 7064–7071. (b) Kleppinger, R.; Lillya, C. P.; Yang, C. *J. Am. Chem. Soc.* **1997**, *119*, 4097–4102. (c) Suárez, M.; Lehn, J. M.; Zimmermann, S. C.; Skoulios, A.; Heinrich, B. *J. Am. Chem. Soc.* **1998**, *120*, 9526–9532.

(23) Ishi-i, T.; Kuwahara, R.; Takata, A.; Jeong, Y.; Sakurai, K.; Mataka, S. *Chem. Eur. J.* **2006**, *12*, 763–776.

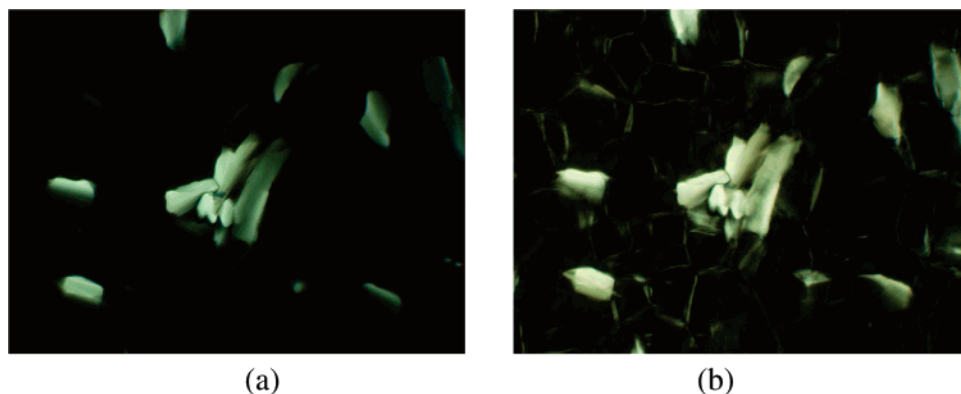


**Figure 5.** Microphotographs of cyclotriphosphazene **5** cooled from the I state (10 °C/min) and taken at (a) 100 °C and (b) 70 °C (same region). A homeotropic region with homogeneously aligned material has been selected to illustrate the texture.

In an effort to confirm the existence of H-bonding in the columnar assemblies, samples of these cyclotriphosphazenes were heated up to the isotropic phase in an FT-IR spectrophotometer and spectra were recorded as a function of decreasing temperature. N–H and amide I ( $\nu_{C=O}$  makes a major contribution) stretching bands are well-known to be sensitive to H-bonding.<sup>24</sup> A set of FT-IR spectra of **5** in these spectral regions at different temperatures and phases is presented in Figure 5. Similar observations were made for the rest of the cyclotriphosphazenes. As can be seen, the  $\nu_{N-H}$  (around 3300  $\text{cm}^{-1}$ ) and amide I (around 1650  $\text{cm}^{-1}$ ) bands clearly indicate the presence of H-bonded (N–H–O=C) amide groups, even in the isotropic state.<sup>25</sup> However, the presence of a shoulder above 3400  $\text{cm}^{-1}$  in the N–H region and a shoulder at around 1680  $\text{cm}^{-1}$  in the amide I region also provide evidence for the coexistence of free amide bands at all temperatures, albeit more intense at higher temperatures.

Furthermore, the broadness of the hydrogen-bonded N–H band and the observation of several peaks in the amide I region at around 1650  $\text{cm}^{-1}$  reflect a distribution of hydrogen-bonded N–H–O=C groups of varying strengths dictated by distance and geometry. Indeed, in the amide I region peaks at 1645, 1649, and 1657 were detected. Besides, an increase of the intensity of the peaks at lower frequencies is detected on cooling from the isotropic state which reveals more intense H-bonds. This situation is also supported by the fact that the H-bonded N–H band shifts toward lower frequencies with decreasing temperature (Figure 6b).

On the other hand, an IR spectrum of compound **5** was also recorded in a dilute hexane solution ( $1 \times 10^{-3}$  M) and only a single, sharp peak with a maximum at 1646  $\text{cm}^{-1}$  was detected in the amide I region (together with a single band at 3311  $\text{cm}^{-1}$  in the N–H region); these bands are probably due to intramolecular H-bonds between the different arms of the same cyclotriphosphazene unit. The corresponding band at 1645  $\text{cm}^{-1}$  in the neat sample may be responsible for stabilizing the discotic structure,<sup>26</sup> while the rest of the

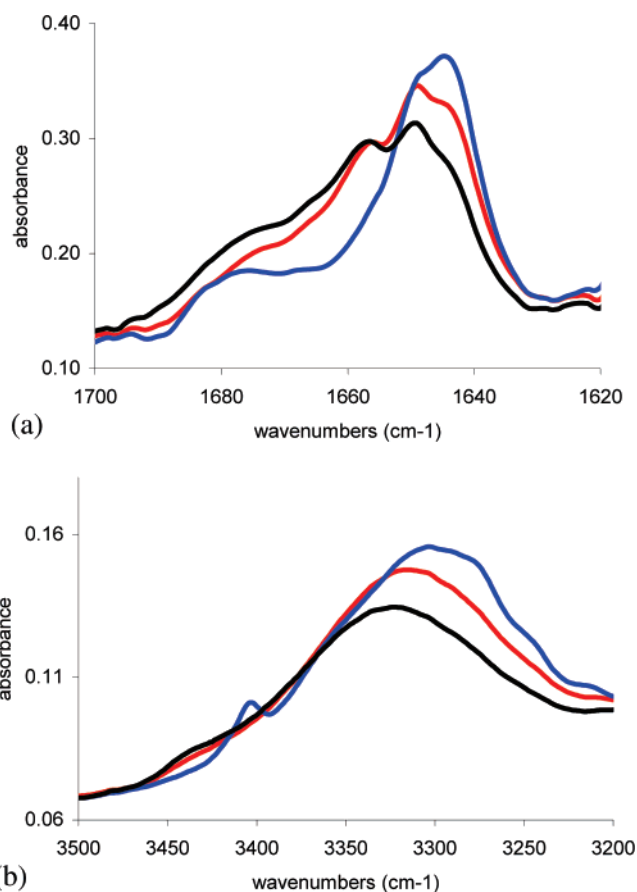


**Figure 6.** FT-IR spectra corresponding to compound **5** in the spectral region of the amide I band (a) and N–H band (b) recorded at different temperatures on cooling from the isotropic state: 150 °C (black), 100 °C (red), and 50 °C (blue).

amide I bands may correspond to intermolecular H-bonds which are involved in the stabilization of the columnar assembly of discotic units. In the isotropic state, the increase in intensity of free amide bands and the marked decrease in the band corresponding to intramolecular H-bonds must be associated with a higher conformational disorder, a situation that leads to the collapse of the discotic structure of the cyclotriphosphazene and, consequently, of the columnar assembly.

**Structural Characterization.** Compounds **3**, **4**, and **5** were studied by X-ray diffraction with the aim of verifying

(24) Xue, C.; Jin, S.; Weng, X.; Ge, J. J.; Shen, Z.; Shen, H.; Graham, J. J.; Jeong, K. U.; Huang, H.; Zhang, D.; Guo, M.; Harris, F. W.; Cheng, S. Z. D. *Chem. Mater.* **2004**, *16*, 1014–1025 and references therein.  
 (25) Skrovaneck, D. J.; Howe, S. E.; Painter, P. C.; Coleman, M. M. *Macromolecules* **1985**, *18*, 1676–1683.  
 (26) See for instance: Palmans, A. R. A.; Vekemans, J. A. J. M.; Fischer, H.; Hikmet, R. A.; Meijer, E. W. *Chem. Eur. J.* **1997**, *3*, 300.

**Table 2. X-ray Diffraction Data for the Mesophases of Cyclotriphosphazenes 3–5**

compd	temp	phase	$d_{\text{obs}}$ (Å)	$d_{\text{calc}}$ (Å)	hk	lattice constants (Å)
3	r.t.	Col <sub>h</sub>	27.7	27.7	1 0	$a = 32.0$
			15.9	16.0	1 1	
			14.0	13.9	2 0	
			10.4	10.5	2 1	
				4.3 <sup>a</sup>		
	142 °C	Col <sub>h</sub>	27.7	27.7	1 0	$a = 32.0$
			16.0	16.0	1 1	
			13.8	13.9	2 0	
10.6			10.5	2 1		
			4.45 <sup>a</sup>			
4	r.t.	Col <sub>h</sub>	32.1	32.0	1 0	$a = 38.0$
			18.5	18.5	1 1	
			16.1	16.0	2 0	
			12.0	12.1	2 1	
5	r.t.	Col <sub>r</sub>	36.1	36.0	2 0	$a = 72$
			34.3	34.3	1 1	$b = 39$
						4.4 <sup>a</sup>
	100 °C	Col <sub>h</sub>	34.4	34.4	1 0	$a = 39.7$

<sup>a</sup> Diffuse maximum. In addition, there are middle-angle diffuse maxima related to the helical order (see text).

the type of mesophase and to determine the structural parameters.

At room temperature, the diffractogram of compound **3** contains a set of four sharp maxima at small angles with reciprocal spacings in the ratio  $1:\sqrt{3}:\sqrt{4}:\sqrt{7}$  (see Table 2 and Figure 7a). In the large-angle region a diffuse scattering halo was obtained at  $1/4.3 \text{ \AA}^{-1}$ . This kind of pattern is unambiguously characteristic of a hexagonal columnar (Col<sub>h</sub>) mesomorphic structure (hexagonal lattice constant is  $a = 32.0 \text{ \AA}$ ). The absence of other X-ray maxima and the diffuse character of the large-angle ring rules out the existence (or coexistence) of a crystalline phase. The tendency to crystallize by annealing above  $T_g$ , found in the DSC study, was confirmed by the X-ray diffractogram recorded on a sample annealed at 110 °C for 1 h. This pattern contained a large number of maxima consistent with a 3D crystalline phase. On melting, this crystalline phase gave rise to a mesophase whose X-ray pattern, taken at 142 °C (Table 2), is very similar to those recorded at room temperature.

The powder diffractograms of compound **4** recorded at room temperature were also consistent with a columnar hexagonal mesophase (both on virgin and annealed samples). Four small-angle reflections were found with reciprocal spacings in the ratio  $1:\sqrt{3}:\sqrt{4}:\sqrt{7}$ , and the hexagonal lattice constant deduced from these spacings is  $a = 37.0 \text{ \AA}$ . In the large-angle region a diffuse scattering halo is obtained at  $1/4.4 \text{ \AA}^{-1}$ .

The room-temperature diffractograms of compound **5** contain two equally spaced sharp maxima at small angles and a set of diffuse scattering maxima at middle and large angles, the most intense of which is observed at  $1/4.4 \text{ \AA}^{-1}$  (see Table 2 and Figure 7b). The absence of Bragg spots (apart from the small-angle maxima) and the diffuseness of the rest of the rings is consistent with a liquid crystal phase. The presence of two equidistant small-angle maxima (the

second of which is much weaker than the first) could be indicative of several types of mesophase, such as smectic or columnar. However, the columnar nature of the phase is clear on the basis of the textures observed by POM (see above). The spacing corresponding to the strong reflection is about  $35 \text{ \AA}$ . A similar X-ray pattern was obtained at 100 °C (above the mesophase–mesophase transition detected by DSC and POM) except for the disappearance of the small-angle second-order reflection and one of the diffuse bands, as well as the shift of the inner reflection and the outer diffuse halo to slightly larger angles. However, the mesophase at higher temperature was clearly characterized as hexagonal columnar on the basis of its optical textures (see above). The deduced hexagonal lattice constant  $a$  at 100 °C is  $39.7 \text{ \AA}$ . In an effort to provide an explanation for the phase transition observed at 87 °C by POM and DSC, high-resolution X-ray measurements at small angles (SAXS) were performed.

The results of these measurements confirmed the previous results for the virgin sample and for the high-temperature mesophase. However, when the sample was heated up to the isotropic liquid and cooled down to room temperature, the peak observed at  $35 \text{ \AA}$  splits into two overlapped maxima corresponding to spacings of  $36.1$  and  $34.3 \text{ \AA}$ , respectively (Figure 8). Assuming that these maxima are the (20) and (11) reflections, respectively, from a 2D rectangular lattice, the deduced lattice constants are  $a = 72 \text{ \AA}$  and  $b = 39 \text{ \AA}$ . This model is supported by the calculated cross-sectional area of each column for the Col<sub>r</sub> mesophase,  $72 \times 39/2 = 1404 \text{ \AA}^2$ , a value similar to that deduced for the Col<sub>h</sub> mesophase, which is  $(\sqrt{3}/2)39.7^2 = 1366 \text{ \AA}^2$ .<sup>27</sup> Furthermore, it can be observed that the  $b$  constant of the Col<sub>r</sub> mesophase ( $39 \text{ \AA}$ ) is practically identical to the  $a$  constant of the Col<sub>h</sub> mesophase ( $39.7 \text{ \AA}$ ). Thus, the Col<sub>r</sub>–Col<sub>h</sub> transition could be viewed as a distortion of the  $ab$  plane. The transition involves a shortening of the rectangular lattice along the  $a$ -axis. This structural model is supported by the SAXS measurements made at 70 °C. At this temperature the two maxima are closer to each other; the resulting lattice constants are  $a = 69 \text{ \AA}$  and  $b = 39 \text{ \AA}$ , and the  $a/b$  ratio is lower than that at room temperature. At the transition to the Col<sub>h</sub> mesophase, the two maxima merge and the  $a/b$  ratio becomes exactly  $\sqrt{3}$ .

Further insight into the mesophase structure was achieved with mechanically aligned samples. Well-oriented patterns were obtained for compound **5** and contained spots distributed in the equator and meridian region (see Figure 7c). In the case of **3** the alignment method was unsuccessful and for **4** only partially oriented patterns could be obtained. In the equatorial region of the pattern of compound **5** (plane perpendicular to the shearing direction) a set of two sharp spots was observed that correspond to the equally spaced small-angle reflections observed in the powder patterns. This result confirms that, as expected in discotic materials, the column axes align parallel to the shearing direction whereas

(27) The (20) and (11) reflections are commonly the innermost and strongest reflections observed in the X-ray patterns of rectangular columnar mesophases. Although in principle the two reflections could also have been indexed in the opposite order, i.e., as (11) and (20), respectively, for this indexation the cross-section area  $S$  of the Col<sub>r</sub> would be too large:  $a = 68.6 \text{ \AA}$ ,  $b = 42.5 \text{ \AA}$ ,  $S = 1458 \text{ \AA}^2$ .

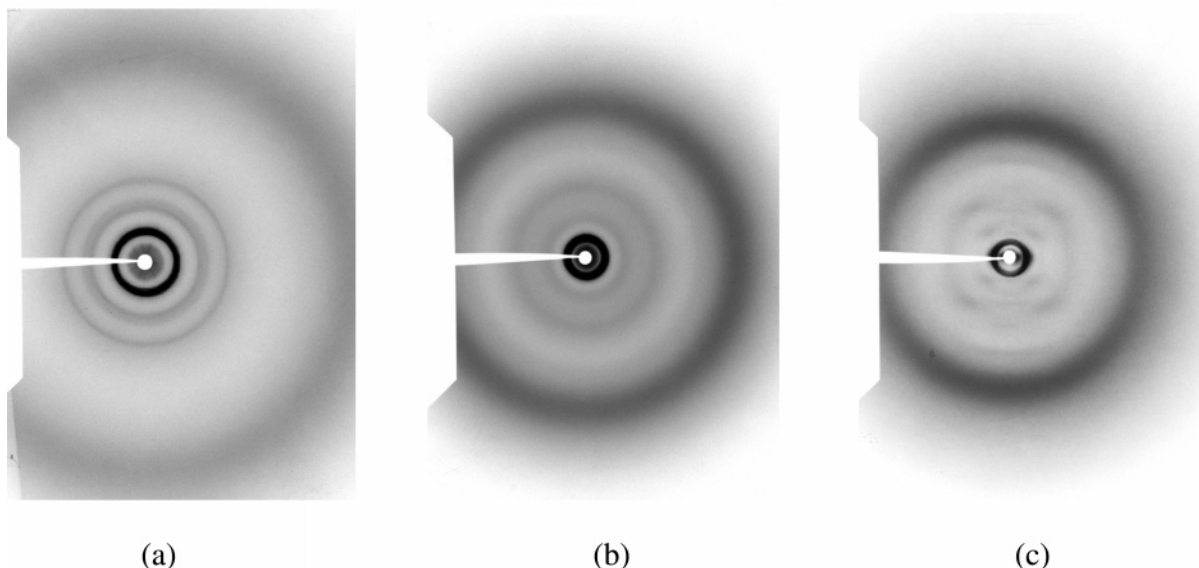


**Figure 7.** (a) X-ray pattern of compound **3** at room temperature (sample-film distance 120 mm). (b) X-ray pattern of compound **5** at room temperature (sample-film distance 80 mm). (c) X-ray pattern of an aligned sample of compound **5** (sample-film distance 60 mm). The capillary axis is vertical.

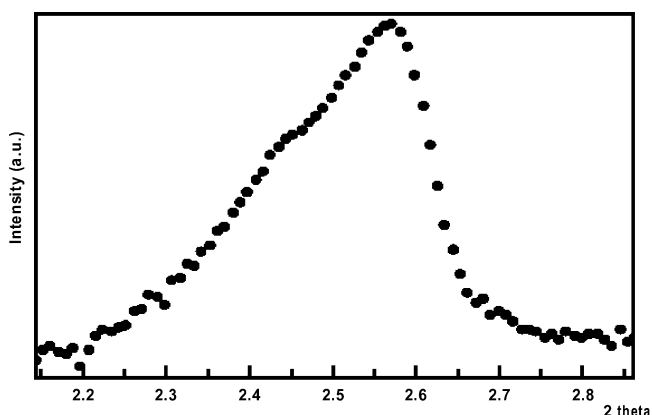


**Figure 8.** SAXS pattern of compound **5** at room temperature.

the 2D lattice lies perpendicular to this direction. The meridian region contains a number of diffuse spots, which are located on equidistant layer lines parallel to the equator. These spots correspond to the middle-angle diffuse maxima found in the powder patterns. The first and second layers exhibit a pair of off-meridian diffuse spots that make up a cross-like pattern. All of these features are consistent with a columnar mesophase with helical order in which the stacking direction and the helical axis are parallel to the meridian (shearing direction).<sup>28</sup> This kind of pattern has also been observed in an analogous cyclotriphosphazene.<sup>14</sup> In compound **5** the diffuse layer lines are spaced by  $1/24 \text{ \AA}^{-1}$ , and this suggests that there is a modulation of the electron density along the helical axis with a period of  $24 \text{ \AA}$ . Taking into account the 3-fold symmetry of this kind of molecule, the helical pitch must in fact be  $3 \times 24 \text{ \AA} = 72 \text{ \AA}$ . The average stacking distance can be deduced from the presence of a scattering maximum centered on the meridian at  $1/6.0 \text{ \AA}^{-1}$  and located at the fourth layer line. The resulting density

( $0.93 \text{ g cm}^{-3}$ ) for this structure, which consists of a two-dimensional rectangular array of columns with lattice constants  $a = 72 \text{ \AA}$  and  $b = 39 \text{ \AA}$  and a stacking distance of  $6.0 \text{ \AA}$ , is a reasonable value and is typical of similar organic molecules. Comparing the stacking distance to the helical pitch, it is deduced that a complete turn must take place after 12 molecules.

In addition to the above-mentioned off-meridian scattering, there is a set of middle-angle diffuse spots centered on the meridian. One of these spots corresponds to a distance of about  $16 \text{ \AA}$ . A similar diffuse spot located approximately at the same place ( $15.5 \text{ \AA}$ ) in the case of the analogous cyclotriphosphazenes bearing mesogenic units with ester groups<sup>14</sup> was assigned to some kind of local order consisting of stacking of “blocks” of about three molecules. Moreover, in the pattern shown in Figure 7c additional diffuse spots along the meridian are located at the same layer lines as the off-meridian spots. These features, not observed in other helical systems,<sup>28</sup> probably arise from the fact that in cyclotriphosphazenes the electronic density is high at the column core, due to the presence of the phosphorus atoms.

In the case of compound **4**, although the degree of alignment was not as good as that for compound **5**, the small-angle spots are reinforced in the equatorial region. Some diffuse bands, with a high azimuthal spread, spaced by about  $1/22 \text{ \AA}^{-1}$  along the meridian direction, were detected at middle angles and these also suggest the existence of helical order in this compound. When these same arguments used for **5** are followed, in this case a helical pitch of  $22 \times 3 = 66 \text{ \AA}$  can be proposed.

## Conclusions

The synthesis of a series of supermolecular liquid crystals based on a cyclotriphosphazene as the dendritic core has been successfully accomplished. These materials show a high thermal stability and columnar mesomorphism over a wide temperature range. Furthermore, the length of the terminal alkyl chains determines the morphology of the materials at

(28) (a) Levelut, A. M. *J. Phys. Lett.* **1979**, *40*, 81. (b) Levelut, A. M.; Oswald, P.; Ghanem, A.; Malthête, J. *J. Phys.* **1984**, *745*. (c) Levelut, A. M.; Malthête, J.; Collet, A. *J. Phys.* **1986**, *47*, 351. (d) Livolant, F.; Levelut, A. M.; Doucet, J.; Benoit, J. P. *Nature* **1989**, *339*, 724. (e) Barberá, J.; Cavero, E.; Lehmann, M.; Serrano, J. L.; Sierra, T.; Vázquez, J. T. *J. Am. Chem. Soc.* **2003**, *125*, 4527.

room temperature. Thus, compounds **3** and **4** give rise to mesomorphic glasses at room temperature but compound **3** can be crystallized by annealing above the  $T_g$ . The increase in the length of the terminal chains in compound **5** gives rise to mesomorphism at room temperature. An IR study of these materials at variable temperatures indicates that intramolecular H-bonding (between arms of the same cyclotriphosphazene) stabilizes the discotic structure adopted by these molecules to optimize the space-filling properties. Furthermore, intermolecular H-bonding (between arms of different cyclotriphosphazenes) also stabilizes the columnar assembly, which results in high clearing transition temperatures. The structural characterization of the columnar mesophase was carried by X-ray diffraction and this revealed helical ordering of cyclotriphosphazenes through the columnar assembly. The great versatility of cyclotriphosphazenes and their thermal stability opens up new possibilities for the design of columnar assemblies at room temperature, in the mesophase or in a vitrified solid state. Such compounds would be of interest for applications in material science.

### Experimental Section

**General Data.**  $K_2CO_3$  and  $Cs_2CO_3$  were dried at 140 °C prior to use. Acetone and tetrahydrofuran were distilled (from anhydrous  $CaSO_4$  and sodium, respectively) under a dry argon atmosphere. Hexachlorocyclotriphosphazene [ $N_3P_3Cl_6$ ] (Stream Chemicals) was purified by recrystallization from hot hexane and dried in vacuo.  $NET_3$  and 4-acetamidophenol were purchased from Aldrich and acid chlorides were prepared by literature methods.<sup>29</sup> All reactions were carried out under a dry argon atmosphere.

Instrumentation and general experimental techniques (elemental analysis, LSIMS, thermogravimetry, and light polarized optical microscopy) were performed as described earlier.<sup>30</sup>  $^1H$ ,  $^{13}C\{^1H\}$ , and  $^{31}P\{^1H\}$  NMR spectra were recorded on a Bruker AV 400 spectrometer. Chemical shifts are quoted relative to  $SiMe_4$  ( $^1H$  and  $^{13}C$ , external) and  $H_3PO_4$  (85%) ( $^{31}P$ , external). MALDI-TOF MS, DSC, X-ray diffraction techniques,<sup>14</sup> and high-resolution SAXS<sup>31</sup> were also obtained as described in the literature. Aligned samples for X-ray diffraction measurements were obtained through mechanical shearing by scratching the inner wall of the capillary tube containing the sample with a glass or metal rod at a temperature close to the transition to the isotropic liquid. The sample was then allowed to cool quickly to room temperature.

FT-IR spectra, collected in the Experimental Section, were recorded from Nujol mulls of as-prepared compounds. FT-IR spectra at different temperatures were taken on KBr pellets, previously heated to the isotropic state, as an average of 128 spectra at a resolution of 2  $cm^{-1}$  on an Nicolet Avatar 360 spectrophotometer together with a Specac accessory for measurements at different temperatures.

**Synthesis of [ $N_3P_3(OC_6H_4\{NHC(O)CH_3\}-4)_6$ ] (**1**).** A mixture of [ $N_3P_3Cl_6$ ] (0.347 g, 1 mmol), 4-acetamidophenol (1.088 g, 7.2 mmol), and  $K_2CO_3$  (1.492 g, 10.8 mmol) in acetone (60 mL) was heated under reflux for 4 days. The volatile materials were

evaporated in vacuo and the residue was washed with water (3 × 20 mL), ethanol (2 × 5 mL), and hexane (3 × 5 mL). The resulting white solid (**1**) was dried in vacuo at 40 °C for 48 h. Yield: 0.9 g (87%).

Elemental analysis. Calcd (%) for  $C_{48}H_{48}N_9O_{12}P_3 + 6H_2O$  (1143.98): C, 50.40; H, 5.29; N, 11.02. Found: C, 50.17; H, 4.97; N, 10.81. IR (KBr): 3301  $cm^{-1}$  (s, br), 3142 (m), 3074  $cm^{-1}$  (m) (N–H); 1668  $cm^{-1}$  (vs) (C=O); 1196 (vs,br), 1177  $cm^{-1}$  (vs,br) (P=N); 955  $cm^{-1}$  (s) (P–O).  $^{31}P\{^1H\}$  NMR (DMSO):  $\delta$  10.31 (s, 3P;  $N_3P_3$  ring).  $^1H$  NMR (DMSO):  $\delta$  9.92 (s, 1H; NH), 7.44 (“d”,  $N = 8.1$  Hz, 2H;  $OC_6H_4N$ ), 6.80 (“d”,  $N = 8.1$  Hz, 2H;  $OC_6H_4N$ ), 2.04 (s, 3H;  $CH_3$ ). MS (LSIMS<sup>+</sup>)  $m/z$  (%): 1053 (8) [ $M + H_2O$ ]<sup>+</sup>, 1036 (100) [ $M + H$ ]<sup>+</sup> and peaks resulting from the loss of C(O)CH<sub>3</sub>, NHC(O)CH<sub>3</sub>, and  $OC_6H_4\{NHC(O)CH_3\}$ .

**Synthesis of [ $N_3P_3(OC_6H_4\{NH_2\}-4)_6$ ] (**2**).** To a solution of **1** (0.518 g, 0.5 mmol) in methanol (20 mL) was added a solution of NaOH (2.4 g) in water (3 mL), and the mixture was heated under reflux for 24 h. The resulting white solid (compound **2**) was filtered off and washed with a large excess of water, ethanol (3 × 5 mL), and hexane (3 × 5 mL) and dried in vacuo at 40 °C for 48 h. Yield: 0.27 g (70%).

Elemental analysis. Calcd (%) for  $C_{36}H_{36}N_9O_6P_3 + 2H_2O$  (819.69): C, 52.75; H, 4.92; N, 15.38. Found: C, 52.90; H, 4.97; N, 15.51. IR (Nujol): 3458 (w), 3436 (m), 3412 (w), 3340 (s,br), 3202  $cm^{-1}$  (s,br) (N–H); 1199(vs,br), 1177  $cm^{-1}$  (vs,br) (P=N); 965  $cm^{-1}$  (s) (P–O).  $^{31}P\{^1H\}$  NMR ( $(CD_3)_2CO$ ):  $\delta$  10.85 (s, 3P;  $N_3P_3$  ring).  $^1H$  NMR ( $(CD_3)_2CO$ ): 6.58 (m, 4H;  $OC_6H_4N$ ), 4.46 (br, 2H;  $NH_2$ ). MS (LSIMS<sup>+</sup>)  $m/z$  (%): 801 (9) [ $M + H_2O$ ]<sup>+</sup>, 784 (100) [ $M + H$ ]<sup>+</sup> and peaks resulting from the successive loss of  $NH_2$ ,  $C_6H_4NH_2$ , and  $OC_6H_4NH_2$ .

**Synthesis of [ $N_3P_3(OC_6H_4\{NHC(O)C_6H_2(3,4,5-(OC_nH_{2n+1})_3-4)_6$ ] ( $n = 6$ ) (**3**) **10** (**4**), **12** (**5**)).** To a solution of **2** (0.157 g, 0.2 mmol) in tetrahydrofuran (15 mL) was added the corresponding acid chloride  $ClC(O)C_6H_2(3,4,5-(OC_nH_{2n+1})_3)$  (1.56 mmol, 0.688 g for **3**, 0.950 g for **4**, or 1.082 g for **5**) and  $NET_3$  (7.8 mmol, 1.1 mL), and the mixture was stirred for 48 h at room temperature. The resulting precipitated  $[NHET_3]Cl$  was filtered off and washed with tetrahydrofuran (2 × 3 mL). The volatile materials were evaporated in vacuo and the residue was washed with acetone (4 × 10 mL) in the case of **5** and with methanol (4 × 10 mL) in the cases of **3** and **4**. The resulting white solids were dried in vacuo at 40 °C for 48 h.

**3** (0.54 g, yield: 84%). Elemental analysis. Calcd (%) for  $C_{186}H_{276}N_9O_{30}P_3$  (3211.21): C, 69.57; H, 8.66; N, 3.93. Found: C, 69.48; H, 8.82; N, 3.81. IR (Nujol): 3298  $cm^{-1}$  (m,br) (N–H); 1645  $cm^{-1}$  (s) (C=O); 1197 (vs,br), 1174  $cm^{-1}$  (vs,br) (P=N); 955  $cm^{-1}$  (s) (P–O).  $^{31}P\{^1H\}$  NMR ( $CDCl_3$ ):  $\delta$  10.42 (s, 3P;  $N_3P_3$  ring).  $^1H$  NMR ( $CDCl_3$ ):  $\delta$  8.83 (br, 1H; NH), 7.35 (“d”,  $N = 6.9$  Hz, 2H;  $OC_6H_4N$ ), 7.17 (s, 2H;  $C_6H_2(OC_6H_{13})_3$ ), 6.88 (“d”,  $N = 6.9$  Hz, 2H;  $OC_6H_4N$ ), 3.97 (br, 2H;  $OCH_2$ ), 3.86 (br, 4H;  $OCH_2$ ), 1.74–1.3 (m, 24H;  $CH_2$ ), 0.88 (br, 9H;  $CH_3$ ).  $^{13}C\{^1H\}$  NMR ( $CDCl_3$ ):  $\delta$  166.52 (1C; C(O)); 153.29, 134.86, 122.90, 120.89 (6C;  $OC_6H_4N$ ); 147.04, 141.56, 129.28, 105.97, (6C;  $C_6H_2(OC_6H_{13})_3$ ); 73.52 (1C;  $OCH_2$ ); 69.26 (2C;  $OCH_2$ ); 31.86, 31.71, 30.45, 29.41, 25.87, 22.70 (12C;  $CH_2$ ); 14.09 (s, 3C;  $CH_3$ ). MS (MALDI-TOF)  $m/z$ : 3211.2 [ $M^+$ ], 3232.2 [ $M + Na$ ]<sup>+</sup>.

**4** (0.59 g, yield: 70%). Elemental analysis. Calcd (%) for  $C_{258}H_{420}N_9O_{30}P_3$  (4221.15): C, 73.41; H, 10.03; N, 2.99. Found: C, 73.37; H, 9.92; N, 3.01. IR (Nujol): 3307  $cm^{-1}$  (m,br) (N–H); 1645  $cm^{-1}$  (s) (C=O); 1196 (vs,br), 1175  $cm^{-1}$  (vs,br) (P=N); 954  $cm^{-1}$  (s) (P–O).  $^{31}P\{^1H\}$  NMR ( $CDCl_3$ ):  $\delta$  10.48 (s, 3P;  $N_3P_3$  ring).  $^1H$  NMR ( $CDCl_3$ ):  $\delta$  8.87 (br, 1H; NH), 7.38 (“d”,  $N = 8.4$  Hz, 2H;  $OC_6H_4N$ ), 7.17 (s, 2H;  $C_6H_2(OC_{10}H_{21})_3$ ), 6.90 (“d”,  $N = 8.4$  Hz, 2H;  $OC_6H_4N$ ), 3.97 (t,  $J(H,H) = 6$  Hz, 2H;  $OCH_2$ ), 3.86

(29) Furniss, B. S.; Hannaford, A. J.; Smith, P. W. G.; Tatchell, A. R. *Vogel's Textbook of Practical Organic Chemistry*; Pearson-Prentice Hall: Essex, 1989; p 692.

(30) (a) Abizanda, D.; Crespo, O.; Gimeno, M. C.; Jiménez, J.; Laguna, A. *Chem. Eur. J.* **2003**, *9*, 3310–3319. (b) Adell, J. M.; Alonso, M. P.; Barberá, J.; Oriol, L.; Piñol, M.; Serrano, J. L. *Polymer* **2003**, *44*, 7829–7841.

(31) Folcia, C. L.; J. Etxebarria, J.; Ortega, J.; Ros, M. B. *Phys. Rev. E* **2005**, *72*, 041709-1–041709-5.



( $t, {}^3J(\text{H,H}) = 6$  Hz, 4H;  $\text{OCH}_2$ ), 1.76–1.26 (m, 48H;  $\text{CH}_2$ ), 0.88 (br, 9H;  $\text{CH}_3$ ).  ${}^{13}\text{C}\{^1\text{H}\}$  NMR ( $\text{CDCl}_3$ ):  $\delta$  166.56 (1C;  $\text{C}(\text{O})$ ); 153.25, 134.83, 122.94, 120.84 (6C;  $\text{OC}_6\text{H}_4\text{N}$ ); 147.03, 141.53, 129.26, 105.96, (6C;  $\text{C}_6\text{H}_2(\text{OC}_{10}\text{H}_{21})_3$ ); 73.52 (1C;  $\text{OCH}_2$ ); 69.24 (2C;  $\text{OCH}_2$ ); 32.04, 30.57, 29.90, 29.82, 29.78, 29.66, 29.51, 26.28, 22.78 (24C;  $\text{CH}_2$ ); 14.17 (s, 3C;  $\text{CH}_3$ ). MS (MALDI-TOF)  $m/z$ : 4220.9 [ $\text{M}^+$ ], 4242.7 [ $\text{M} + \text{Na}^+$ ].

**5** (0.718 g, yield: 76%). Elemental analysis. Calcd (%) for  $\text{C}_{294}\text{H}_{492}\text{N}_9\text{O}_{30}\text{P}_3$  (4726.12): C, 74.72; H, 10.49; N, 2.67. Found: C, 74.89; H, 10.89; N, 2.51. IR (Nujol): 3257  $\text{cm}^{-1}$  (m,br) (N–H); 1643  $\text{cm}^{-1}$  (s) (C=O); 1197 (vs,br), 1175  $\text{cm}^{-1}$  (vs,br) (P=N); 956  $\text{cm}^{-1}$  (s) (P–O).  ${}^{31}\text{P}\{^1\text{H}\}$  NMR ( $\text{CDCl}_3$ ):  $\delta$  10.49 (s, 3P;  $\text{N}_3\text{P}_3$  ring).  ${}^1\text{H}$  NMR ( $\text{CDCl}_3$ ):  $\delta$  8.88 (br, 1H;  $\text{NH}$ ), 7.34 (“d”,  $N = 8.1$  Hz, 2H;  $\text{OC}_6\text{H}_4\text{N}$ ), 7.17 (s, 2H;  $\text{C}_6\text{H}_2(\text{OC}_{12}\text{H}_{25})_3$ ), 6.87 (“d”,  $N = 8.1$  Hz, 2H;  $\text{OC}_6\text{H}_4\text{N}$ ), 3.96 (br, 2H;  $\text{OCH}_2$ ), 3.84 (br, 4H;

$\text{OCH}_2$ ), 1.74–1.26 (m, 60H;  $\text{CH}_2$ ), 0.88 (br, 9H;  $\text{CH}_3$ ).  ${}^{13}\text{C}\{^1\text{H}\}$  NMR ( $\text{CDCl}_3$ ):  $\delta$  166.52 (1C;  $\text{C}(\text{O})$ ); 153.28, 134.84, 122.88, 120.91 (6C;  $\text{OC}_6\text{H}_4\text{N}$ ); 147.03, 141.56, 129.32, 105.94, (6C;  $\text{C}_6\text{H}_2(\text{OC}_{12}\text{H}_{25})_3$ ); 73.53 (1C;  $\text{OCH}_2$ ); 69.29 (2C;  $\text{OCH}_2$ ); 32.04, 30.56, 29.83, 29.67, 29.51, 26.28, 22.79 (30C;  $\text{CH}_2$ ); 14.19 (s, 3C;  $\text{CH}_3$ ). MS (MALDI-TOF)  $m/z$ : 4749 [ $\text{M} + \text{Na}^+$ ].

**Acknowledgment.** This work was supported by the Spanish-FEDER projects MAT2005-06373-C02-01, CTQ2004-04118-C02-01/BQU, and Gobierno de Aragón. Dr. César L. Folcia (University of the Basque Country) is gratefully acknowledged for the SAXS measurements and helpful discussions.

CM061147D